

The Telomerase/Vault-associated Protein TEP1 Is Required for Vault RNA Stability and Its Association with the Vault Particle

Valerie A. Kickhoefer,* Yie Liu,[§] Lawrence B. Kong,[‡] Bryan E. Snow,[§] Phoebe L. Stewart,[‡] Lea Harrington,[§] and Leonard H. Rome*

*Department of Biological Chemistry and Jonsson Comprehensive Cancer Center, and [‡]Department of Molecular and Medical Pharmacology, Crump Institute for Molecular Imaging, University of California at Los Angeles, School of Medicine, Los Angeles, California 90095; [§]Ontario Cancer Institute/Amgen Institute, Department of Medical Biophysics, University of Toronto, Toronto, Ontario M5G 2C1, Canada

Abstract. Vaults and telomerase are ribonucleoprotein (RNP) particles that share a common protein subunit, TEP1. Although its role in either complex has not yet been defined, TEP1 has been shown to interact with the mouse telomerase RNA and with several of the human vault RNAs in a yeast three-hybrid assay. An *mTep1*^{-/-} mouse was previously generated which resulted in no apparent change in telomere length or telomerase activity in six generations of *mTep1*-deficient mice. Here we show that the levels of the telomerase RNA and its association with the telomerase RNP are also unaffected in *mTep1*^{-/-} mice. Although vaults purified from the livers of *mTep1*^{-/-} mice appear structurally intact by both negative stain and cryoelectron microscopy,

three-dimensional reconstruction of the *mTep1*^{-/-} vault revealed less density in the cap than previously observed for the intact rat vault. Furthermore, the absence of TEP1 completely disrupted the stable association of the vault RNA with the purified vault particle and also resulted in a decrease in the levels and stability of the vault RNA. Therefore, we have uncovered a novel role for TEP1 in vivo as an integral vault protein important for the stabilization and recruitment of the vault RNA to the vault particle.

Key words: TEP1 • vaults • mouse embryonic stem cells • RNA stability • cryo-EM

Introduction

Mammalian vaults are large cytoplasmic RNP complexes, composed of at least four components: the 104-kD major vault protein (MVP),¹ the 193-kD poly(ADP-ribosyl) polymerase VPARP, the telomerase/vault-associated protein TEP1, and one or more small RNAs (vRNAs) (Kedersha and Rome, 1986). Identification of VPARP as a functional poly(ADP-ribose) polymerase (PARP) provided the first evidence of a vault-associated enzymatic activity (Kickhoefer et al., 1999a). The recent discovery of TEP1 as an associated protein in both vaults and telomerase provides an intriguing link between these two RNP complexes that is not yet understood (Harrington et al., 1997a; Kickhoefer et al., 1999b). Vaults are widely distrib-

uted throughout eukaryotes and have a distinct morphology that is highly conserved (for reviews see Rome et al., 1991; Kickhoefer et al., 1996). Although the function of the vault particle has remained elusive, several studies suggest that it may be involved in some form of intracellular transport (Scheffer et al., 1995; Hamill and Suprenant, 1997; Abbondanza et al., 1998; Herrmann et al., 1999; Kitazono et al., 1999).

Purified vaults display an eightfold barrel-like symmetry where the barrel is formed of multiple copies of the MVP, with caps on each end postulated to contain VPARP, TEP1, and the vRNAs (Kedersha et al., 1991; Kong et al., 2000). Cryoelectron microscopy (cryo-EM) image reconstruction of the 13-MD vault particle purified from rat liver shows the interior of the particle to be hollow, lending support to a role as a carrier (Kong et al., 1999). Recently, a reconstruction of RNase-treated vaults localized the vRNA to the caps of the vault particle by difference mapping (Kong et al., 2000). vRNAs have been cloned from humans, rats, mice, and bullfrogs and their length varies from 86 to 141 bases. Humans and bullfrogs contain multiple related vRNAs (Kickhoefer et al., 1993, 1998).

Address correspondence to Valerie A. Kickhoefer, Department of Biological Chemistry, UCLA School of Medicine and Jonsson Comprehensive Cancer Center, Los Angeles, CA 90095-1737. Tel.: (310) 794-4873. Fax: (310) 206-5272. E-mail: vkick@mednet.ucla.edu

¹Abbreviations used in this paper: ES, embryonic stem; hTR, human telomerase RNA; MEF, mouse embryonic fibroblast; mTR, mouse telomerase RNA; MVP, major vault protein; mVR, mouse vault RNA; PARP, poly(ADP-ribose) polymerase; RT, reverse transcription; TERT, telomerase reverse transcriptase; TRAP, telomere repeat amplification protocol.

Previously we have shown that several of the human vRNAs, in addition to the telomerase RNA, specifically interact with TEP1 in the yeast RNA-protein interaction assay (Harrington et al., 1997a; Kickhoefer et al., 1999b). Although purified vaults contain TEP1, they do not possess telomerase activity (Kickhoefer et al., 1999b).

Most eukaryotic chromosome ends are maintained by telomerase, a multisubunit RNP complex that uses an RNA template to specify the addition of telomeric DNA onto the chromosome ends (for review see Greider, 1996). The essential role of the telomerase RNA component in providing a template for telomere DNA synthesis is well established in eukaryotes. Biochemical studies indicate that the human telomerase complex is >1 MD, suggesting that it contains numerous subunits in addition to the telomerase catalytic component, telomerase reverse transcriptase (TERT), and the human telomerase RNA (hTR) (Nakayama et al., 1997; Schnapp et al., 1998). TEP1 was initially identified as the mammalian homologue of the *Tetrahymena* telomerase p80 protein (Harrington et al., 1997a; Nakayama et al., 1997). Immunoprecipitates of TEP1 possess telomerase activity and TEP1 is associated with TERT and hTR (Harrington et al., 1997a,b; Nakayama et al., 1997). In vitro, the minimal complex necessary for reconstitution of telomerase activity appears to comprise TERT and hTR and does not require the addition of TEP1 (Weinrich et al., 1997; Beattie et al., 1998; Holt et al., 1999).

Homologous recombination has been used to disrupt the gene encoding *mTep1* (Liu et al., 2000). Despite the fact that TEP1 is associated with the telomerase RNA and the telomerase catalytic subunit TERT in vivo, *mTep1*-deficient mice showed no significant alteration in telomerase activity or telomere length (Liu et al., 2000). Here we show that biochemical fractionation of the telomerase complexes and the level of telomerase RNA in cell extracts showed no detectable alterations in *mTep1*-deficient mice. Since TEP1 is not unique to the telomerase complex, we analyzed the effect on the integrity of the vault particle and its associated RNA, vRNA. Gross vault morphology appears to be unaltered in *mTep1*-deficient mice, as observed by both negative stain and cryo-EM. A three-dimensional reconstruction of *mTep1*-deficient vaults revealed less density in the cap and supports the localization of at least a portion of TEP1 to the ends of the vault caps, placing it next to the assigned location of vRNA. The absence of TEP1 disrupted vRNA association with vaults and led to a decrease in steady state levels of vRNA in all tissues examined. This decreased stability was reflected in a decrease in the half-life of the vRNA. These data suggest that TEP1 is important for vRNA binding and recruitment to the vault complex, and that the vRNA association with TEP1 and/or the vault complex appears to stabilize the vRNA.

Materials and Methods

mTep1-deficient Mice, Embryonic Stem Cells, and Mouse Embryonic Fibroblasts

The generation of *mTep1*^{-/-} homozygous animals has been described elsewhere (Liu et al., 2000). A founder breeding pair of generation four *mTep1*^{-/-} mice of mixed genetic background (129SvJ/C57BL) were used to establish a colony at the University of California at Los Angeles. The

generation five mice were interbred to produce generation six offspring. All mice used in this study were from generation six *mTep1*^{-/-} animals. embryonic stem (ES) cell clones were generated from G418-resistant *mTep1*^{+/-} ES cell clones by culturing with an increased G418 concentration (4 mg/ml) (Liu et al., 2000). Mouse embryonic fibroblast (MEF) cell lines were obtained using the 3T3 protocol (Todaro and Green, 1963). MEF 5 and 8 are two independent lines derived from *mTep1*^{-/-} mouse embryos and MEF 11 cells were derived from a wild-type mouse embryo. All three MEF lines were derived from the same litter.

Cell Lysate Preparation, Partial Purification of Mouse Telomerase, Telomerase Assays, and Quantitative Reverse Transcription PCR Analysis of Mouse Telomerase RNA

S-100 extracts from cultured ES cells were prepared as described (Prowse et al., 1993). Approximately 37 mg of protein from each sample was applied to Sephacryl S-400 (Amersham Pharmacia Biotech) equilibrated in 2.3× hypobuffer (23 mM Hepes, pH 8.0, 7 mM KCl, 2.3 mM MgCl₂ including 1 mM DTT, RNase, and protease inhibitors). Individual fractions from each sample were measured for telomerase activity and the presence of mouse telomerase RNA (mTR). Telomerase activity was assayed using the telomere repeat amplification protocol (TRAP) (Kim et al., 1994) following the manufacturer's instructions (Intergen, Inc.). TRAP was performed on the individual fractions from each sample for 20 PCR cycles. The amount of mTR in each fraction was determined by a real time quantitative reverse transcription (RT)-PCR analysis (Taqman) using ABI Prism 7700 Sequence Detection System (PE Biosystems). The sequences of the PCR primers are 5'-GCCGCAAGGACAGGAATG, 3'-GGGTGCACCTCCACAGC, and TGGTCCCCGTGTTCCGGTGTCTTACC (probe).

Vault Purification and Analysis

Vaults were purified from mouse liver as described previously (Kong et al., 1999). However, the procedure was significantly scaled down due to the limited quantities and size of mouse livers. Approximately 5–6 g of mouse liver was used and all gradient steps were carried out using the AH650 rotor (Sorvall) at 25,000 rpm. In the final purification step, vaults were purified over a single cesium chloride gradient to minimize sample loss, and the purified vaults were pelleted at 100,000 g using the Ti80 rotor (Beckman Coulter) and resuspended in ~125 μl of 0.09 M MES, pH 6.5 containing PMSF. Purified vaults (20 μl) were analyzed by SDS-PAGE followed by silver staining or immunoblot analysis. All antibodies (anti-MVP, anti-VPARP, and anti-TEP1) have been described previously and were used accordingly (Kickhoefer et al., 1999a,b). EM of uranyl acetate stained vaults was carried out as described previously (Kedersha and Rome, 1986).

RNA Isolation and Northern Analysis

Total RNA was isolated from various tissues or MEF cell lines using RNA STAT (Tel-test, Inc.) following the manufacturer's protocol. Total RNA (25 μg) was fractionated on 6% acrylamide–8 M urea gel, electroblotted to Zeta-Probe GT membrane (Bio-Rad Laboratories), and hybridized with the indicated probes according to the manufacturer's instructions. Probes were prepared by random priming with the Prime-It II kit (Stratagene). The mTR probe is based on the wild-type mTR sequence (Blasco et al., 1995). The mouse vault RNA (mVR) probe is based on the mouse (Balb/c) vault RNA gene sequence (data available from GenBank/EMBL/DDBJ under accession no. AY007237). Hybridizations were carried out sequentially; membranes were stripped and hybridized to an end-labeled oligonucleotide complementary to the mouse 5S RNA gene (AACCATGCCCGACCCTGCTTAGCTTC) to use as a loading control. For actinomycin D (Sigma-Aldrich) experiments, the MEF cells were incubated in fresh medium containing a 10-μg/ml concentration of the drug. At the indicated times total RNA was isolated.

Cryo-EM and Image Processing

A 20-μl sample of vaults purified from *mTep1*^{-/-} mouse livers was used for cryo-EM. Holey carbon grids were glow discharged and then 4 μl of the vault sample was applied to each grid, blotted with filter paper, and then plunged into ethane slush chilled by liquid nitrogen (Adrian et al., 1984). Digital micrographs were collected on a Philips CM120 transmission electron microscope equipped with an LaB6 filament, Gatan cryo-accessories, and a Gatan slow-scan CCD camera (1,024 × 1,024 pixels, YAG scintillator). The nominal microscope magnification was 45,000, yielding a digital pixel size of 4.1 Å on the molecular scale. All images were collected

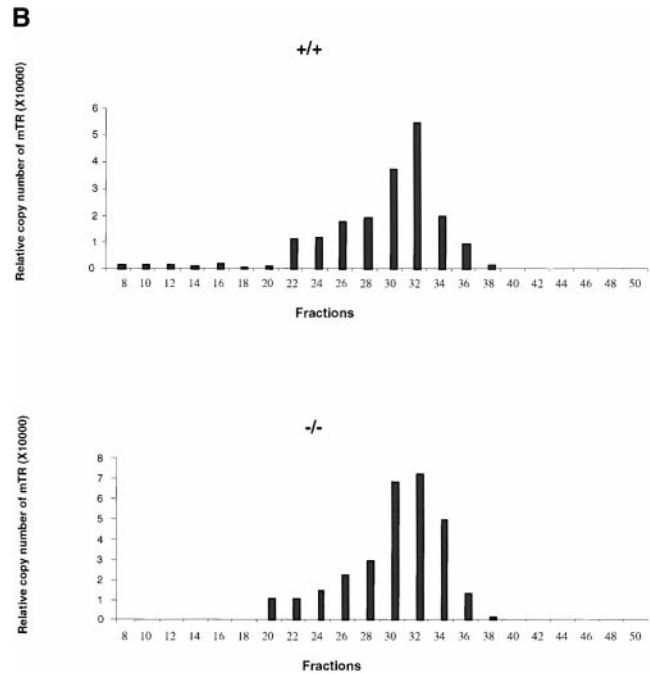
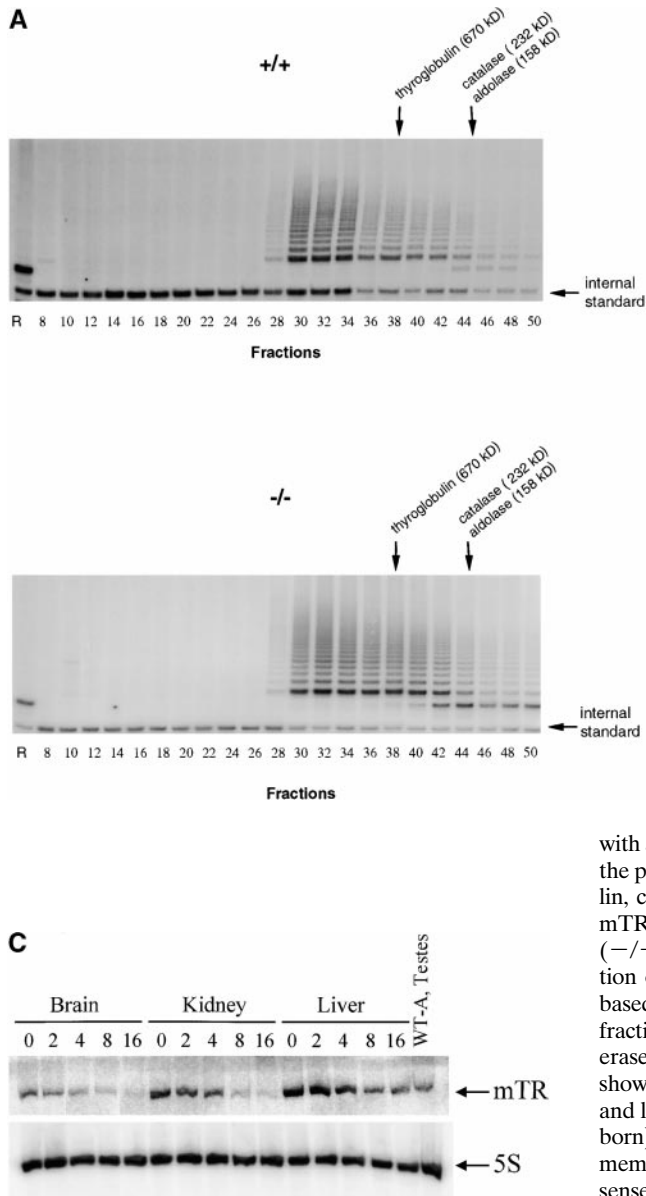


Figure 1. mTR expression in *mTep1*^{-/-} mice. (A) Telomerase activity in the individual Sephacryl S-400 fractions of wild-type (+/+) and *mTep1*-deficient (-/-) ES cell lysates. TRAP was performed for 20 PCR cycles on 5 μ l of each fraction of the indicated genotype. An internal PCR standard for the TRAP is shown at bottom right with an arrow. R represents the RNase A treatment of 5 μ l of the fraction with the peak telomerase activity. Peak fractions of the sizing standards thyroglobulin, catalase, and aldolase are indicated above. (B) RT-PCR quantitation of mTR in the individual fractions of wild-type (+/+) and *mTep1*-deficient (-/-) ES cell lysates. The Taqman assay was performed on 5 μ l of each fraction of the indicated genotype. The relative copies of mTR were calculated based on a standard curve using serial diluted mouse, total RNA, and/or the fraction with the peak telomerase activity. The fraction with the peak telomerase activity had no detectable mTR after the RNase A treatment (data not shown). (C) Northern blot analysis of total RNA prepared from brain, kidney, and liver tissue at the indicated postnatal developmental stages (day 0 is newborn). As a control, total RNA from adult wild-type testes was prepared. The membrane was probed with mTR (top), stripped, and re-probed with an anti-sense 5S oligonucleotide as a loading control (bottom).

with a defocus value of $-1.0 \mu\text{m}$ giving a first CTF zero of 19 \AA . CTF correction was carried out as described previously (Kong et al., 2000).

Image processing was performed on DEC/Compaq alpha workstations and a Silicon Graphics Reality Monster supercomputer with 32 processors. The QVIEW software package (Shah and Stewart, 1998) was used to extract individual vault particle images into 200×200 pixel fields. A preliminary set of 305 particle images was used to calculate Euler angles using the angular reconstitution method in the IMAGIC software package (van Heel et al., 1996). Initially cyclic eightfold symmetry was assumed and a preliminary reconstruction was calculated with imposed cyclic eightfold symmetry. This reconstruction showed strong features of dihedral eightfold symmetry, implying that the upper and lower halves of the vault are related by a twofold symmetry axis. Thus dihedral eightfold symmetry was imposed during the subsequent refinement cycles. The third and final refinement cycle was performed with a 4° anchor set spacing and a 1° refinement step size. The resolution of the final reconstruction, which was based on 397 particle images, was 27 \AA as assessed by the Fourier shell correlation 0.5 threshold criterion (Böttcher et al., 1997; Conway et al., 1997).

A linear ramped elliptical mask was used during refinement of the vault to remove internal contents as well as external noise surrounding the particle. The inner ellipse had dimensions of 151 and 306 \AA ; the outer ellipse radii were 224 and 413 \AA . The isosurface and the density slab representations were generated using the AVS software package (Advanced Visual Systems, Inc.). To select an appropriate isosurface level, the molecular mass of the *mTep1*^{-/-} vault was assumed to be 11.8 MD. This mass

value was estimated from the average STEM mass measurement of 12.9 MD for the intact vault (Kedersha et al., 1991), minus 5% for the vRNA (0.64 MD) and the mass of two copies of TEP1 (0.48 MD).

Results

mTep1 Is Not Essential for mTR Processing, Stability, or Association with Telomerase Complexes

Analysis of telomerase complexes from *mTep1*^{-/-} and wild-type ES cells indicated that the absence of TEP1 did not grossly affect the fractionation properties of telomerase complexes when examined by S-400 chromatography (Fig. 1 A). Fractions were analyzed for telomerase activity using the TRAP (Kim et al., 1994). Both wild-type and *mTep1*-deficient telomerase activities paralleled each other with activities spread from fraction 28–50. No detectable change in mTR fractionation with telomerase complexes was observed using quantitative RT-PCR (Fig. 1 B). The slightly higher telomerase activity and higher copy number of telomerase RNA from the *mTep1*-defi-

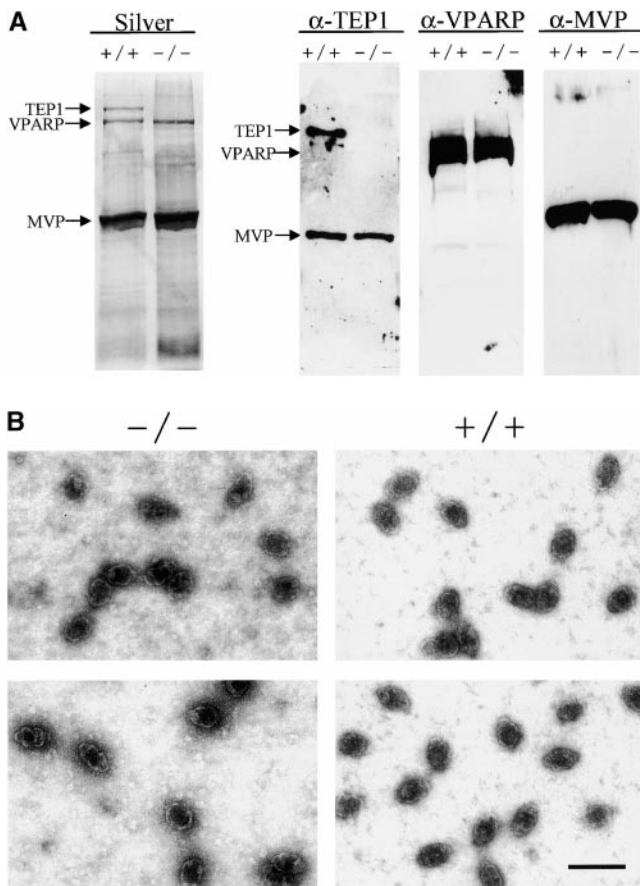


Figure 2. Purified vaults. (A) Silver stain of vaults purified from livers of either wild-type (+/+) or *mTep1*-deficient (-/-) mice (arrows indicate TEPI, VPARP, and MVP). The identities of the vault proteins were confirmed by immunoblot analysis using the indicated antibodies (α -TEPI, α -VPARP, and α -MVP). Due to limited sample availability immunoblots were stripped and re-probed with the different antibodies. Consequently, the MVP antibody was not completely removed and MVP reappeared in subsequent re-probing with TEPI antibodies. As expected, TEPI is absent in the *mTep1*-deficient mice. The anti-VPARP antibody was made against a portion of the human VPARP protein and recognizes the mouse VPARP protein here as a smear. (B) Electron micrographs of negatively stained vaults purified from either wild-type (+/+) or *mTep1*-deficient (-/-) mice. Bar, 100 nm.

cient ES fractions in Fig. 1, A and B, were not reproducible. In other experiments, we did not observe a difference in the level of telomerase RNA or activity between the wild-type and *mTep1*-deficient ES cells (Liu, Y., and L. Harrington, data not shown). Since both telomerase complex fractionation and mTR levels are unaffected in *mTep1*-deficient ES cells, we next determined whether the developmental profile of mTR expression varied in *mTep1*^{-/-} mice. Total RNA was isolated from brain, kidney, and liver from *mTep1*^{-/-} mice at different postnatal development stages up to 16 d after birth (Fig. 1 C). mTR RNA was expressed in all tissues examined at birth and decreased rapidly after birth in *mTep1*^{-/-} mice, while 5S RNA levels remained unchanged. These results are similar to the previously published developmental RNA profile of mTR in wild-type mice where mTR levels also rapidly declined postnatally (Blasco et al., 1995).

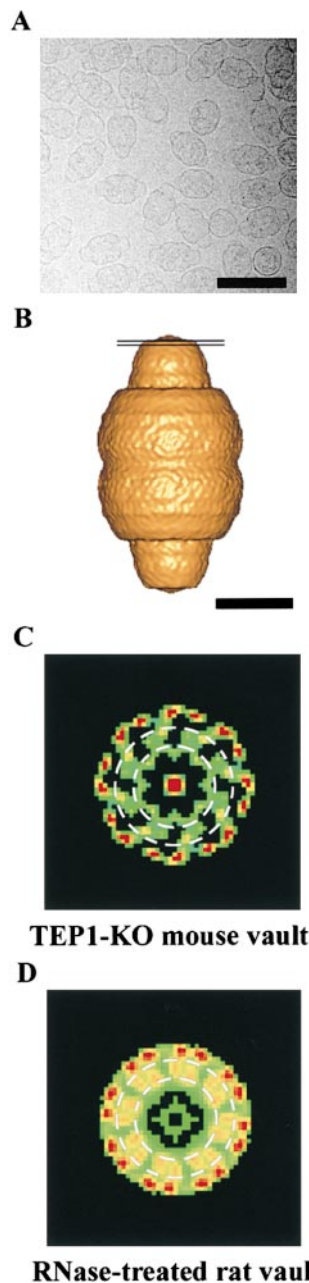


Figure 3. Cryo-EM reconstruction of vaults purified from *mTep1*-deficient mice. (A) A portion (640 × 640 pixels) of a digital cryoelectron micrograph of the vaults. (B) A surface representation of the final reconstruction at 27 Å resolution. The two black lines indicate the position of the density slab shown in C. (C) A two-dimensional projection of a density slab through the top of the cap of the *mTep1*^{-/-} vault reconstruction. KO, knockout. (D) The corresponding density slab from the RNase-treated rat vault reconstruction (Kong et al., 2000). The dashed white circles in C and D outline the intermediate ring region in which a major difference is observed between the two reconstructions. Bars: (A) 1,000 Å; (B) 250 Å.

Vaults Isolated from *TEPI*^{-/-} Mice Appear Structurally Intact

To ascertain the role of TEPI in vault particle formation in vivo, we purified vaults from the livers of wild-type and *mTep1*^{-/-} mice (see Materials and Methods). Vault levels, composition, and structure (assayed by negative stain EM) remained constant in all wild-type mouse strains tested (C57BL, 129SvJ, and Balb/c; data not shown). Vault components from *mTep1*^{-/-} mice purified with identical properties as wild-type vaults through a series of gradient and centrifugation steps (data not shown). Gel electrophoresis and silver staining of highly purified vault fractions from *mTep1*^{-/-} and wild-type mouse livers showed comparable amounts of MVP and VPARP (Fig. 2 A, Silver), whereas the *mTep1*^{-/-} vault preparation, as expected, lacked TEPI (Fig. 2 A, Silver). The absence of TEPI in the vault preparation from *mTep1*^{-/-} mice was also confirmed by immu-

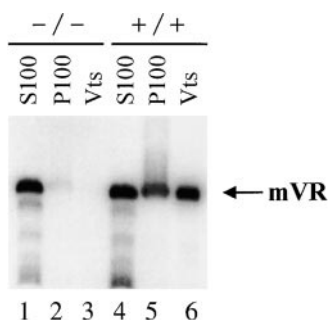


Figure 4. Vault RNA association with vaults. Northern analysis of RNA purified from subcellular fractions during vault purification from wild-type (+/+) and *mTep1*-deficient (-/-) mice. S100 (100,000 g supernatant, lanes 1 and 4), P100 (100,000 g pellet, lanes 2 and 5), and purified vaults (Vts, lanes 3 and 6).

noblotting of the purified vaults with antibodies against each individual vault protein component (anti-MVP, anti-VPARP, and anti-TEP1 antibodies, Fig. 2 A). Due to limited sample availability immunoblots were stripped and reprobed with the different antibodies. Consequently, the MVP antibody was not completely removed and MVP reappeared in subsequent reprobing with the anti-TEP1 antibody. As expected, TEP1 is absent in the *mTep1*-deficient mice (Liu et al., 2000). EM of negatively stained purified preparations from mouse liver showed that vault structures from the *mTep1*^{-/-} mice were indistinguishable from those purified from wild-type mice (Fig. 2 B).

Cryo-EM Reconstruction of *mTep1*^{-/-} Vault Reveals Reduced Cap Density

Purified *mTep1*^{-/-} vaults were flash frozen on holey carbon EM grids and cryoelectron micrographs were collected (Fig. 3 A). Images of 397 vault particles were computationally combined to generate a three-dimensional reconstruction of the *mTep1*^{-/-} vault at 27-Å resolution. A surface representation of the reconstruction (Fig. 3 B) shows that the overall structure of the *mTep1*^{-/-} vault is similar to that of both the intact and RNase-treated rat vaults (Kong et al., 1999, 2000). Careful examination of the density slices revealed that the strong cap density attributed to the vRNA is lacking in the reconstruction of the *mTep1*^{-/-} vault. When the *mTep1*^{-/-} vault and the RNase-treated rat vault reconstructions are compared, minor differences are found throughout the structures that are probably attributable to subtle variations between species. However, a major difference between the two reconstructions is observed in a density slab through the top of the cap (Fig. 3 B). Within this slab, both reconstructions show the same pattern of 16 strong density spots around the outermost edge. However, less density is observed in the mouse *Tep1*^{-/-} vaults within an intermediate ring (Fig. 3, C and D). This difference likely corresponds to the position of the TEP1 protein at the end of the vault cap, a location for TEP1 previously predicted from structural modeling (Kong et al., 2000).

mTep1 Is Essential for Stable Interaction of Vault RNAs with the Vault Particle

We next examined the purified vault fractions for the presence of associated vRNA. Previously it has been shown that the vRNA is not required for the structural integrity of the vault particle (Kedersha et al., 1991; Kong et al., 2000). Northern blot analysis revealed the complete absence of vRNA in vaults purified from *mTep1*^{-/-} mice

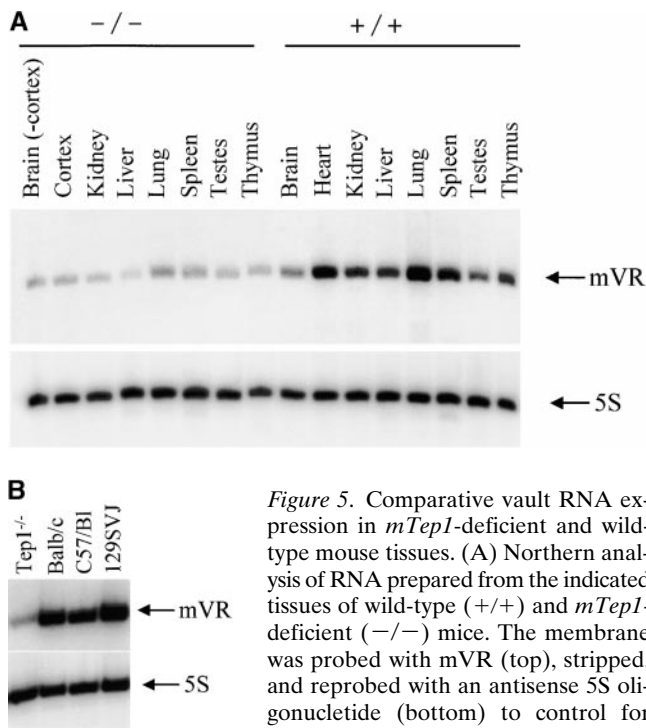


Figure 5. Comparative vault RNA expression in *mTep1*-deficient and wild-type mouse tissues. (A) Northern analysis of RNA prepared from the indicated tissues of wild-type (+/+) and *mTep1*-deficient (-/-) mice. The membrane was probed with mVR (top), stripped, and reprobed with an antisense 5S oligonucleotide (bottom) to control for loading. (B) Northern analysis of RNA

prepared from different mice strains as indicated, and probed as indicated above. mVR expression does not vary significantly in the different wild-type strain backgrounds.

compared with wild-type vaults (Fig. 4, compare lanes 3 and 6). Since vault purification takes several days to complete, we were concerned about the possibility that the vRNA was degraded during the isolation procedure. To test this possibility we examined early fractions during vault purification for the presence of the vRNA. Vaults are known to pellet at 100,000 g (P100) and previous studies have shown that the vRNA is present in both the P100 and the supernatant (S100) fractions (Kickhoefer et al., 1998). Northern analysis indicated that as expected the vRNA is present in both S100 and P100 fractions with about twice as much RNA associated with the S100 fraction compared with the P100 in the wild-type mice (Fig. 4, lanes 4 and 5). In contrast, only a trace amount of vRNA is present in the P100 extract from the livers of *mTep1*^{-/-} mice (Fig. 4, lane 2). However, the amount of vRNA in the S100 extract from the *mTep1*-deficient mice is comparable to that seen in wild-type mice S100 extract (Fig. 4, lanes 1 and 4). These data support the hypothesis that TEP1 is responsible for the vRNAs stable association with the vault particle and suggest that vRNA levels may be altered in *mTep1*-deficient mice.

A comparison of vRNA levels in *mTep1*^{-/-} and wild-type mouse tissues revealed vRNA levels to be three- to fivefold lower in *mTep1*-deficient mice (Fig. 5 A). One explanation for this variable expression level could be due to a difference in vRNA levels between wild-type mice (C57BL/6) and the mixed genetic background of the *mTep1*-deficient mice (Liu et al., 2000). Several mouse strains were analyzed to determine whether vRNA levels varied, and no difference was found (Fig. 5 B). The blots were stripped and hybridized for 5S RNA as a loading control (Fig. 5, A and B). 5S RNA levels also do not vary

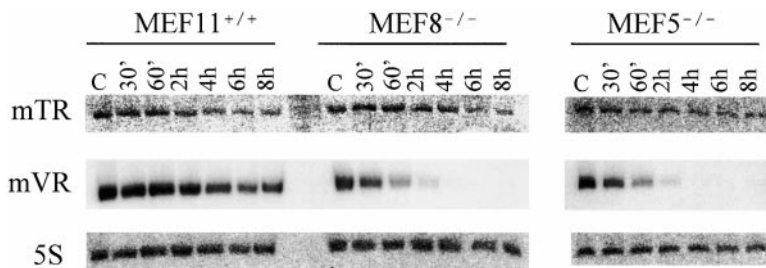


Figure 6. Vault RNA expression varies in actinomycin D-treated MEFs. Northern analysis of RNA prepared from wild-type (MEF11^{+/+}) and *mTep1*-deficient (MEF8^{-/-} and MEF5^{-/-}) cells treated with actinomycin D for the indicated times. The membrane was probed with mTR (top), stripped, and reprobbed first with mVR (middle) and next with an antisense 5S oligonucleotide (bottom). Control (C) samples were not treated with drug.

between the *mTep1*^{-/-} and wild-type mice. These data suggested that the lower steady state level of vRNA might be due to a change in the stability of the vRNA in the *mTep1*^{-/-} mice.

To analyze the stability of the vRNA we used several MEF cell lines obtained using the 3T3 protocol (Todaro and Green, 1963). MEF 5 and 8 are two independent lines derived from *mTep1*^{-/-} mouse embryos, MEF 11 cells are derived from a wild-type mouse embryo, and all three MEF lines are derived from the same litter. MEF cells were treated with actinomycin D to inhibit transcription and total RNA was isolated at different time intervals after drug treatment (30 min, 1, 2, 4, 6, and 8 h). Northern analysis revealed that the vRNAs stability is reduced in the *mTep1*^{-/-} MEF lines compared with the wild-type MEF lines. In wild-type MEF cells, vRNA has a half-life of 4–6 h; however, in both *mTep1*^{-/-} MEF lines, the vRNAs half-life is reduced to 0.5–1 h (Fig. 6, mVR). The blots were stripped and reprobbed with either mTR or 5S (a loading control). No effect is seen on the stability of the mTR (Fig. 6). However, previous analysis has suggested that the telomerase RNA possesses a half-life of 24 h or longer; therefore, under these experimental conditions a subtle effect on mTR half-life may not be detected (Yi et al., 1999).

Discussion

We have found that in the absence of TEPI the vRNA is no longer stably associated with vaults. In addition, the apparent half-life of the vRNA is reduced by severalfold. In contrast, the association of mTR with telomerase activity and the developmental expression profile of mTR was unaltered. TEPI has been shown to interact with mTR and several human vRNAs using the yeast RNA–protein interaction assay and its association with hTR in vivo has been demonstrated (Harrington et al., 1997a,b; Nakayama et al., 1997; Kickhoefer et al., 1999b). Apparently, the absence of TEPI has no obvious effect on telomerase activity, telomere length, or the levels of mTR in vivo (Liu et al., 2000). If TEPI were associated with only a fraction of the mTR in the cell, its disruption might have no phenotypic consequences in vivo. Alternatively, other telomerase RNA binding proteins may share a redundant role with TEPI in telomerase complex assembly. In support of this hypothesis is the recent identification of two additional telomerase RNA binding proteins, hStau and L22. Each of these proteins immunoprecipitates telomerase activity and hTR, but not each other or TEPI, suggesting that there may be multiple functional telomerase complexes (Le et al., 2000).

Although the role of TEPI in the telomerase complex appears to be redundant, its function in the vault complex is

not. At least six independent vault preparations have been carried out on *mTep1*-deficient mice and the vault proteins purified with properties identical to those of wild-type vaults through several centrifugation and gradient fractionations. The vaults from the *mTep1*-deficient mice have the typical lobular morphology as observed by negative stain EM, suggesting that TEPI is not essential for vault particle formation. Previously we proposed that the 16 WD40 repeats of TEPI might play a role in organizing the eightfold symmetry of the vault (Kong et al., 2000), although this does not appear to be the case in light of our data.

To examine the structure of the vault from *mTep1*-deficient mice more closely, we performed cryo-EM and three-dimensional image reconstruction. We noted that the *mTep1*^{-/-} vault was most similar to the RNase-treated rat vault, in which the vRNA was reduced to below detectable levels (Kong et al., 2000). This finding is consistent with our observation that vRNA does not stably associate with the *mTep1*^{-/-} vault. The most significant difference between the *mTep1*^{-/-} vault and the RNase-treated vault was found at the ends of the vault caps. This difference corresponds to the region in the RNase-treated vault reconstruction where we previously observed 16-fold density and modeled the 16 WD40 repeat domain of TEPI (Kong et al., 2000). The reconstruction of the *Tep1*-deficient vault supports the localization of at least a portion of TEPI to the ends of the vault caps, placing it next to the assigned location of vRNA.

We have observed an abrogation of the vRNA in purified vaults from *Tep1*-deficient mice. Our findings indicate that TEPI is a critical protein involved in vRNA binding and that TEPI is largely responsible for localizing and stabilizing vRNA association with vault particles. The role of the vRNA in vault particle function is not yet understood. However, the vRNA is not a structural component, as its degradation does not alter vault structure (Kedersha et al., 1991; Kong et al., 2000). It remains possible that in the *Tep1*-deficient mice the vRNA may partly contribute to vault function, since a small portion of vRNA is present in the 100,000 g pellet (P100) and could be unstably associated with the vault particle. In vaults, TEPI appears to facilitate the vault RNA's localization to the particle.

It is not clear whether the stabilizing effect of TEPI on vRNA is through direct binding or through localizing vRNA to the vault particle where it is subsequently protected from degradation. It is possible that TEPI functions in the localization of other RNAs to RNP complexes. Reduced levels of other small RNAs have been observed for several disrupted RNP complexes. The Sm proteins are required for wild-type levels of U snRNAs (Rymond, 1993; Xue et al., 2000) and the Sm-like proteins are required for U6 snRNA accumulation (Pannone et al., 1998; Mayes et

al., 1999; Salgado-Garrido et al., 1999). Disruption of the gene encoding Ro in *Caenorhabditis elegans* led to reduced levels of Y RNAs in mutant worms (Labbé et al., 1999). Disruption of several of the signal recognition particle proteins in the yeast *Saccharomyces cerevisiae* leads to decreased levels of ScR1 RNA, reduced signal recognition particle protein levels, and inefficient protein translocation across the ER membrane (Brown et al., 1994).

Are the differences in telomerase RNAs and vRNAs the reason TEP1 affects them differently? Each RNA is transcribed by a different class of RNA polymerase. vRNA is transcribed by RNA polymerase III and contains the classical features of a polymerase III gene, including an internal A and B box with a stretch of T's at the 3' end typical for transcription termination (Kickhoefer et al., 1993). In contrast, RNA polymerase II presumably transcribes the hTR and mTR genes (Hinkley et al., 1998; Zhao et al., 1998). Recently, 32 vertebrate telomerase RNAs were analyzed and a phylogenetic comparative analysis predicted a secondary structure that contains four conserved structural domains with 10 helical regions of the RNA being universally conserved (Chen et al., 2000). One of the conserved structural domains contains a sno-RNA Box H/ACA element that is thought to be necessary for telomerase RNA stability, processing, and possibly for assembly into functional telomerase complexes (Mitchell et al., 1999a). Indeed, a portion of telomerase RNA has been localized to the nucleolus and mutation of the Box H/ACA element results in decreased stability of telomerase RNA (Mitchell et al., 1999a; Narayanan et al., 1999). Dyskerin, a component of H/ACA snoRNPs, was recently shown to interact with hTR (Mitchell et al., 1999b). Mutation in the human dyskerin gene leads to decreased steady state levels of hTR, reduced telomerase activity, and shortened telomeres in cells taken from two patients with the disorder dyskeratosis congenita (Mitchell et al., 1999b). However, the level of three other H/ACA snoRNAs was unaffected in the dyskeratosis congenita cells. These data suggest that dyskerin has a role in telomerase RNA biogenesis and possibly in telomerase RNP assembly. The secondary structure of vRNAs has not yet been solved, but all known sequences can be folded into similar structures that contain several stem loops (Kickhoefer et al., 1993; Kickhoefer, V.A., and L.H. Rome, unpublished observations).

There is no obvious sequence conservation between vRNAs and hTR; therefore, it is not yet clear what determines the recognition of telomerase RNA or vRNA by TEP1. It is not yet known whether vRNAs and telomerase RNAs bind to separate sites on TEP1 or compete for binding to the same site. Despite the redundancy of TEP1 in the telomerase complex but not the vault particle, our studies reveal the first phenotype associated with the disruption of TEP1 and provide an important first step in elucidating the physiological role of TEP1 in RNA assembly, localization, and RNP function.

We thank members of the Rome laboratory for critical comments and discussion; Rena Oulton for assistance with gel filtration chromatography; Wen Zhou, Xiaoling Zhang, and Hue Kha for assistance with the Taqman assays; Carol Gray and Donna Crandall for digital imaging; and Hedi Roseboro, and David Yeung for technical assistance.

This work was supported by a US Public Health Service grant from the National Institutes of Health (GM38097 to L.H. Rome) and funding from the University of California BioSTAR Program (V.A. Kickhoefer and

L.H. Rome). P.L. Stewart acknowledges support from the National Science Foundation (MCB-9722353). L. Harrington acknowledges support from the Canadian Institute of Health Research and a US Public Health Service grant from the National Institutes of Health (AG8422117).

Submitted: 23 August 2000

Revised: 2 November 2000

Accepted: 8 November 2000

References

- Abbondanza, C., V. Rossi, A. Roscigno, L. Gallo, A. Belsito, G. Piluso, N. Medici, V. Nigro, A.M. Molinari, B. Monchamont, and G.A. Puca. 1998. Interaction of vault particles with estrogen receptor in the MCF-7 breast cancer cell. *J. Cell Biol.* 141:1301-1310.
- Adrian, M., J. Dubochet, J. Lepault, and A.W. McDowell. 1984. Cryo-electron microscopy of viruses. *Nature.* 308:32-36.
- Beattie, T.L., W. Zhou, M.O. Robinson, and L. Harrington. 1998. Reconstitution of human telomerase activity *in vitro*. *Curr. Biol.* 8:177-180.
- Blasco, M.A., W. Funk, B. Villeponteau, and C.W. Greider. 1995. Functional characterization and developmental regulation of mouse telomerase RNA. *Science.* 269:1267-1270.
- Böttcher, B., S.A. Wynne, and R.A. Crowther. 1997. Determination of the fold of the core protein of hepatitis B virus by electron cryomicroscopy. *Nature.* 386:88-91.
- Brown, J.D., B.C. Hann, K.F. Medzhradszky, M. Niwa, A.L. Burlingame, and P. Walter. 1994. Subunits of the *Saccharomyces cerevisiae* signal recognition particle required for its functional expression. *EMBO (Eur. Mol. Biol. Organ.) J.* 13:4390-4400.
- Chen, J.L., M.A. Blasco, and C.W. Greider. 2000. Secondary structure of vertebrate telomerase RNA. *Cell.* 100:503-514.
- Conway, J.F., N. Cheng, A. Zlotnick, P.T. Wingfield, S.J. Stahl, and A.C. Steven. 1997. Visualization of a 4-helix bundle in the hepatitis B virus capsid by cryo-electron microscopy. *Nature.* 386:91-94.
- Greider, C.W. 1996. Telomere length regulation. *Annu. Rev. Biochem.* 65:337-365.
- Hamill, D.R., and K.A. Suprenant. 1997. Characterization of the sea urchin major vault protein: a possible role for vault ribonucleoprotein particles in nucleocytoplasmic transport. *Dev. Biol.* 190:117-128.
- Harrington, L., T. McPhail, V. Mar, W. Zhou, R. Oulton, M.B. Bass, I. Arruda, and M.O. Robinson. 1997a. A mammalian telomerase-associated protein. *Science.* 275:973-977.
- Harrington, L., W. Zhou, T. McPhail, R. Oulton, D.S. Yeung, V. Mar, M.B. Bass, and M.O. Robinson. 1997b. Human telomerase contains evolutionarily conserved catalytic and structural subunits. *Genes Dev.* 11:3109-3115.
- Herrmann, C., E. Golkaramnay, E. Inman, L. Rome, and W. Volkmann. 1999. Recombinant major vault protein is targeted to neuritic tips of PC12 cells. *J. Cell Biol.* 144:1163-1172.
- Hinkley, C.S., M.A. Blasco, W.D. Funk, J. Feng, B. Villeponteau, C.W. Greider, and W. Herr. 1998. The mouse telomerase RNA 5'-end lies just upstream of the telomerase template sequence. *Nucleic Acids Res.* 26:532-536.
- Holt, S.E., D.L. Aisner, J. Baur, V.M. Tesmer, M. Dy, M. Ouellette, J.B. Trager, G.B. Morin, D.O. Toft, J.W. Shay, W.E. Wright, and M.A. White. 1999. Functional requirement of p23 and hsp90 in telomerase complexes. *Genes Dev.* 13:817-826.
- Kedersha, N.L., and L.H. Rome. 1986. Isolation and characterization of a novel ribonucleoprotein particle: large structures contain a single species of small RNA. *J. Cell Biol.* 103:699-709.
- Kedersha, N.L., J.E. Heuser, D.C. Chugani, and L.H. Rome. 1991. Vaults. III. Vault ribonucleoprotein particles open into flower-like structures with octagonal symmetry. *J. Cell Biol.* 112:225-235.
- Kickhoefer, V.A., R.P. Searles, N.L. Kedersha, M.E. Garber, D.L. Johnson, and L.H. Rome. 1993. Vault ribonucleoprotein particles from rat and bullfrog contain a related small RNA that is transcribed by RNA polymerase III. *J. Biol. Chem.* 268:7868-7873.
- Kickhoefer, V.A., S.K. Vasu, and L.H. Rome. 1996. Vaults are the answer, what is the question? *Trends Cell Biol.* 6:174-178.
- Kickhoefer, V.A., K.S. Rajavel, G.L. Scheffer, W.S. Dalton, R.J. Scheper, and L.H. Rome. 1998. Vaults are up-regulated in multidrug-resistant cancer cell lines. *J. Biol. Chem.* 273:8971-8974.
- Kickhoefer, V.A., A.C. Siva, N.L. Kedersha, E.M. Inman, C. Ruland, M. Streuli, and L.H. Rome. 1999a. The 193-kD vault protein, VPAP, is a novel poly(ADP-ribose) polymerase. *J. Cell Biol.* 146:917-928.
- Kickhoefer, V.A., A.G. Stephen, L. Harrington, M.O. Robinson, and L.H. Rome. 1999b. Vaults and telomerase share a common subunit, TEP1. *J. Biol. Chem.* 274:32712-32717.
- Kim, N.W., M.A. Piatyszek, K.R. Prowse, C.B. Harley, M.D. West, P.L. Ho, G.M. Coviello, W.E. Wright, S.L. Weinrich, and J.W. Shay. 1994. Specific association of human telomerase activity with immortal cells and cancer. *Science.* 266:2011-2015.
- Kitazono, M., T. Sumizawa, Y. Takebayashi, Z.S. Chen, T. Furukawa, S. Nagayama, A. Tani, S. Takao, T. Aikou, and S. Akiyama. 1999. Multidrug resistance and the lung resistance-related protein in human colon carcinoma SW-620 cells. *J. Natl. Cancer Inst.* 91:1647-1653.
- Kong, L.B., A.C. Siva, L.H. Rome, and P.L. Stewart. 1999. Structure of the

- vault, a ubiquitous cellular component. *Structure Fold. Des.* 7:371–379.
- Kong, L.B., A.C. Siva, V.A. Kickhoefer, L.H. Rome, and P.L. Stewart. 2000. RNA location and modeling of a WD40 repeat domain within the vault. *RNA*. 6:890–900.
- Labbé, J.C., S. Hekimi, and L.A. Rokeach. 1999. The levels of the RoRNP-associated Y RNA are dependent upon the presence of ROP-1, the *Caenorhabditis elegans* Ro60 protein. *Genetics*. 151:143–150.
- Le, S., R. Sternglanz, and C.W. Greider. 2000. Identification of two RNA-binding proteins associated with human telomerase RNA. *Mol. Biol. Cell*. 11:999–1010.
- Liu, Y., B.E. Snow, M.P. Hande, G. Baerlocher, V.A. Kickhoefer, D. Yeung, A. Wakeham, A. Itie, D.P. Siderovski, P.M. Lansdorp, M.O. Robinson, and L. Harrington. 2000. The telomerase-associated protein TEP1 is not essential for telomerase activity or telomere length maintenance in vivo. *Mol. Cell. Biol.* 20:8178–8184.
- Mayes, A.E., L. Verdone, P. Legrain, and J.D. Beggs. 1999. Characterization of Sm-like proteins in yeast and their association with U6 snRNA. *EMBO (Eur. Mol. Biol. Organ.) J.* 18:4321–4331.
- Mitchell, J.R., J. Cheng, and K. Collins. 1999a. A box H/ACA small nucleolar RNA-like domain at the human telomerase RNA 3' end. *Mol. Cell. Biol.* 19:567–576.
- Mitchell, J.R., E. Wood, and K. Collins. 1999b. A telomerase component is defective in the human disease dyskeratosis congenita. *Nature*. 402:551–555.
- Nakayama, J., M. Saito, H. Nakamura, A. Matsuura, and F. Ishikawa. 1997. TLP1: a gene encoding a protein component of mammalian telomerase is a novel member of WD repeats family. *Cell*. 88:875–884.
- Narayanan, A., A. Lukowiak, B.E. Jádý, F. Dragon, T. Kiss, R.M. Terns, and M.P. Terns. 1999. Nucleolar localization signals of box H/ACA small nucleolar RNAs. *EMBO (Eur. Mol. Biol. Organ.) J.* 18:5120–5130.
- Pannone, B.K., D. Xue, and S.L. Wolin. 1998. A role for the yeast La protein in U6 snRNP assembly: evidence that the La protein is a molecular chaperone for RNA polymerase III transcripts. *EMBO (Eur. Mol. Biol. Organ.) J.* 17:7442–7453.
- Prowse, K.R., A.A. Avilion, and C.W. Greider. 1993. Identification of a non-processive telomerase activity from mouse cells. *Proc. Natl. Acad. Sci. USA*. 90:1493–1497.
- Rome, L., N. Kedersha, and D. Chugani. 1991. Unlocking vaults: organelles in search of a function. *Trends Cell Biol.* 1:47–50.
- Rymond, B.C. 1993. Convergent transcripts of the yeast PRP38-SMD1 locus encode two essential splicing factors, including the D1 core polypeptide of small nuclear ribonucleoprotein particles. *Proc. Natl. Acad. Sci. USA*. 90:848–852.
- Salgado-Garrido, J., E. Bragado-Nilsson, S. Kandels-Lewis, and B. Séraphin. 1999. Sm and Sm-like proteins assemble in two related complexes of deep evolutionary origin. *EMBO (Eur. Mol. Biol. Organ.) J.* 18:3451–3462.
- Scheffer, G.L., P.L. Wijngaard, M.J. Flens, M.A. Izquierdo, M.L. Slovak, H.M. Pinedo, C.J. Meijer, H.C. Clevers, and R.J. Scheper. 1995. The drug resistance-related protein LRP is the human major vault protein. *Nat. Med.* 1:578–582.
- Schnapp, G., H.P. Rodi, W.J. Rettig, A. Schnapp, and K. Damm. 1998. One-step affinity purification protocol for human telomerase. *Nucleic Acids Res.* 26:3311–3313.
- Shah, A.K., and P.L. Stewart. 1998. QVIEW: software for rapid selection of particles from digital electron micrographs. *J. Struct. Biol.* 123:17–21.
- Todaro, G.J., and H. Green. 1963. Quantitative studies of the growth of mouse embryo cells in culture and their development into established lines. *J. Cell Biol.* 17:299–313.
- van Heel, M., G. Harauz, and E.V. Orlova. 1996. A new generation of the IMAGIC image processing system. *J. Struct. Biol.* 116:17–24.
- Weinrich, S.L., R. Pruzan, L. Ma, M. Ouellette, V.M. Tesmer, S.E. Holt, A.G. Bodnar, S. Lichtsteiner, N.W. Kim, J.B. Trager, et al. 1997. Reconstitution of human telomerase with the template RNA component hTR and the catalytic protein subunit hTERT. *Nat. Genet.* 17:498–502.
- Xue, D., D.A. Rubinson, B.K. Pannone, C.J. Yoo, and S.L. Wolin. 2000. U snRNP assembly in yeast involves the La protein. *EMBO (Eur. Mol. Biol. Organ.) J.* 19:1650–1660.
- Yi, X., V.M. Tesmer, I. Savre-Train, J.W. Shay, and W.E. Wright. 1999. Both transcriptional and posttranscriptional mechanisms regulate human telomerase template RNA levels. *Mol. Cell. Biol.* 19:3989–3997.
- Zhao, J.Q., S.F. Hoare, R. McFarlane, S. Muir, E.K. Parkinson, D.M. Black, and W.N. Keith. 1998. Cloning and characterization of human and mouse telomerase RNA gene promoter sequences. *Oncogene*. 16:1345–1350.